Proceedings of Global Power and Propulsion Society
ISSN-Nr: 2504-4400
GPPS Xi'an21
18th – 20th October, 2021
www.gpps.global

GPPS-TC-2021-0064

AN AERODYNAMIC PERFORMANCE OPTIMIZATION METHOD APPLIED TO THE INTAKE GRILLE OF ACTIVE CLEARANCE CONTROL SYSTEM

Shuyi Zhang
School of Mechanical Engineering,
Shanghai Jiaotong University
homedown.good@163.com
Shanghai, China

Bo Yang
School of Mechanical Engineering,
Shanghai Jiaotong University
byang0626@sjtu.edu.cn
Shanghai, China

Hong Xie
School of Mechanical Engineering,
Shanghai Jiaotong University
369165499@qq.com
Shanghai, China

Guoming Zhu
School of Mechanical Engineering,
Shanghai Jiaotong University
1562161048@qq.com
Shanghai, China

Moru Song
School of Mechanical Engineering,
Shanghai Jiaotong University
Summery0624@163.com
Shanghai, China

ABSTRACT

The active clearance control system (ACC) of turbine is one of the core components,which can reduce the fuel consumption of civil aero-engine. And the tip-clearance change is greatly affected by the aerodynmaic performance of intake grille. To improve the performance, in this work, an aerodynamic optimization method of intake grille is proposed. This method is divided into three parts, such as the parameterization, the fitness evaluation and the optimization algorithm. Based on the commercial software NX 12.0, the grille is parameterized according to seven key geometric parameters. In order to evaluate the aerodynamic performance of grille accurately, a special fitness function is presented and figured out with the help of an adaptive back-propagation multi-layer feedforward artificial neural network (BP-MLANN). Lastly, utilizing the continuous swarm particle optimization-modified very fast simulated annealing algorithm (CPSO-MVFSA), the optimal aerodynamic performance of intake grille is achieved. Through analyzing the aerodynamic experiments and the computational fluid dynamic (CFD) simulation of intake grille, it is found that the aerodynamic performance of the optimized grille is better than that of the original. Therefore, this aerodynamic optimization method is feasible to improve the aerodynamic performance of intake grille.

INTRODUCTION

Gas-turbine which can convert the energy of high temperature and pressure gas flow into mechanical energy, is considered as one of the three core components of aero engine. However, its efficiency, performance and service life are easily affected by blade-tip clearance. Gas-turbine active clearance control (ACC) technology can control the changes of blade-tip clearance to achieve tip clearance as small as possible in the main working state of the engine, so as to improve engine performance, reduce fuel consumption and increase service life (Lattime et al., 2012). Among all feasible ACC methods, the thermal control ACC method is the most widely used. The ACC of high-pressure turbine (HPT) is realized mainly by controlling thermal deformation of turbine casing (Melcher, 2003; ZENG Jun et al., 2012). The turbine casing is usually cooled or heated by the intake airflow with different temperatures from a high-pressure compressor or an external bypass, and then the radial deformation of the casing is achieved.

Generally, the character of thermal control ACC system is mainly divided into two aspects such as the outlet cooling character and the inlet intake character (GU Wei et al., 2013). Some research results about the outlet cooling character of ACC have been published. For example, the outflow characteristics and the heat transfer characteristics of the impinging holes of the cooling pipe with circular section for the ACC system of low-pressure turbine through numerical simulation was studied (Ahmed et al., 2011). The insulating coverage effect of the perforated impact-jet on the surface of casing with

This work is licensed under **Attribution 4.0 International (CC BY 4.0)** See:
https://creativecommons.org/licenses/by/4.0/legalcode

circular cross-section flat cooling air pipe was explored (Da Soghe et al., 2011). Based on some experiments, the influence of different flow modes on the internal heat transfer characteristics of the casing in ACC system of high-pressure turbine was analyzed (Tapanlis et al., 2014). However, very few researches about the inlet intake character of ACC are explored.

With the fast development of the computational technology, some optimization algorithms were presented and used in the aerodynamic optimization of machines. The aerodynamic optimization is usually divided into three important procedures such as the shape parameterization, the fitness value evaluation and the optimization algorithm. The significant improvement of these procedures is meaningful to the effectiveness and efficiency of optimization (Dominic et al., 2015). During the optimization, the dimensions of the design variables are completely determined by the parameterization methods. Good parameterization methods have some similarities, such as the enough flexibility to cover the whole search space, the fewer number of design parameters and the ability to avoid curvature discontinuities at the junctions (Zhihui Li et al., 2017)

Besides the parameterization, the fitness value evaluation is also very important. Due to the fact that the fitness function is related to the aerodynamic performance and the geometrical parameters, the complex flow field simulation calculation is necessary. But the computation consumption could not be stood in every case. To overcome these problems effectively, the concept of surrogate model was adopted in which the complex nonlinear relationship between the parameters and the aerodynamic performance could be built, and used to replace the CFD calculation (Duan, W. et al., 2017). Owing to its great approximation capability, the artificial neural network (ANN) was often as a surrogate model. For the ANN, the approximate capability was mainly influenced by its topology structure (Nazghelichi et al., 2011). To efficiently get the ANN with the appropriate topology structure, some global intelligent optimization methods, such as genetic algorithm (GA) (Yang Z. et al., 2015), simulated annealing (SA) (Zhang S. et al., 2020) and particle swarm optimization (PSO) (Zhang J R. et al., 2007; Zhang S. et al., 2020), were adopted. Although these methods could improve the approximation ability of ANN by optimizing the topology structure to some extent, there was no specific principle to determine a high-efficiency topology.

Due to that the cooling airflow was introduced from the bypass through the intake grille, the aerodynamic performance of intake grille will greatly influence on the inlet intake character of ACC. To improve the aerodynamic performance of intake grille, an improved aerodynamic optimization method is proposed. Firstly, the geometry of intake grille is parameterized through the commercial software NX 12.0. Then the back-propagation multi-layer feedforward artificial neural network (BP-MLFANN) is optimized by an improved hybrid intelligent optimization method and used as a surrogate model to predict the aerodynamic performance of intake grille. Lastly, the continuous swarm particle optimization-modified very fast simulated annealing algorithm (CPSO-MVFSA) is adopted to search for the intake grille with the optimal aerodynamic performance.

AERODYNAMIC OPTIMIZATION METHODOLOGY

Parameterization of Intake Grille

The intake system of ACC is shown in Fig.1 in which the shape of the bypass bottom is arc-shaped and the top surface of intake grille is coplanar with the inner bottom surface. From Fig. 1(a), it is found that some airflow in the bypass is bled to the ACC by the intake grille. Fig. 1(b) displays the intake grille geometry model which owns four arc-shaped blades. In order to realize the geometric deformation of the intake model fast, the intake grille is parameterized by the commercial software NX 12.0 and shown in Fig. 2. Seven key geometric parameters such as the inlet angle α_1 , the outlet angle α_2 , the chord L , the interval 1 I_1 , the interval 2 I_2 , the interval 3 I_3 and the interval 4 I_4 , are selected to describe the geometry of the intake grille.

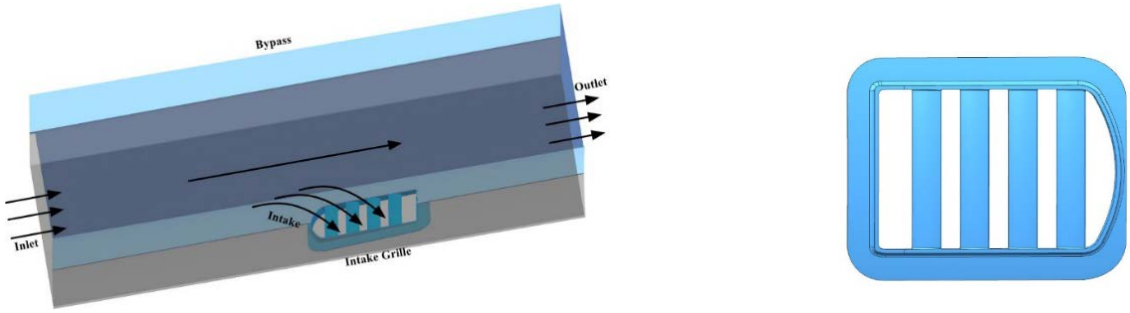

a) Intake b) Intake grille model

Fig.1 The Illustration of ACC Intake System

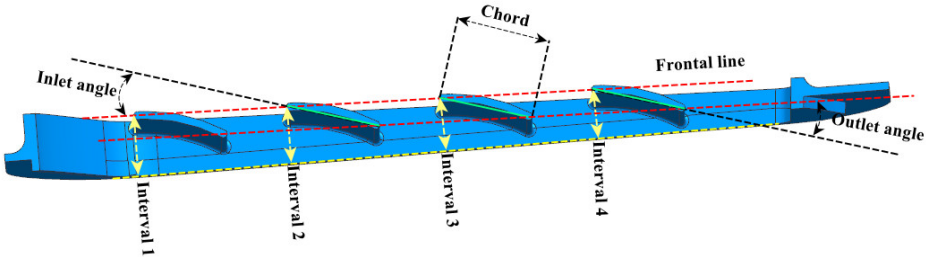

Fig.2 The Parameterization of Intake Grille

Sample Construction and Surrogate Model

Sample construction

According to the abovementioned parameterization, it is known that seven geometric parameters $\alpha_1, \alpha_2, L, I_1, I_2, I_3, I_4$ are selected to optimize the aerodynamic performance of the intake grille. The value ranges of these seven parameters are shown in Eq. (1) in which $\alpha_1^{'}, \alpha_2^{'}, L^{'}, I_1^{'}, I_2^{'}, I_3^{'}, I_4^{'}$ are the original value of intake grille, and they determine the searching space of the geometry of intake grille. In order to guarantee the efficiency of the optimization, the Latin Hypercube Sampling design method is used to generate the uniform samples.

$$\begin{bmatrix} \alpha_1 \\ \alpha_2 \\ L \\ I_1 \\ I_2 \\ I_3 \\ I_4 \end{bmatrix} \in \begin{bmatrix} [0.75, 1.35] \cdot \alpha_1^{'} \\ [0.75, 1.35] \cdot \alpha_2^{1} \\ [0.75, 1.35] \cdot L^{'} \\ [0.75, 1.35] \cdot I_1^{'} \\ [0.75, 1.35] \cdot I_2^{'} \\ [0.75, 1.35] \cdot I_3^{'} \\ [0.75, 1.35] \cdot I_4^{'} \end{bmatrix} \tag{1}$$

In this work, the aerodynamic optimization aims to search for the intake grille with optimal aerodynamic performance. To evaluate the aerodynamic performance of intake grille, two coefficients, such as the total pressure recovery coefficient $Cp_{total} = P_{out}/P_{in}$ and the intake airflow coefficient $\eta_m = Q_{om2}/Q_{im}$ are adopted. And the fitness function of intake grille is proposed and shown in Eq. (2). Larger fitness value presents higher total pressure recovery coefficient and higher intake airflow capability. On account of the control variables and the corresponding fitness values, the samples of the aerodynamic performance of intake grille are constructed.

$$\begin{aligned} f = {} & c_1 \left(\frac{Cp_{total} - \left(\frac{P_{out2}}{P_{in}} \right)_{ref}}{\left(\frac{P_{out2}}{P_{in}} \right)_{ref}} \right) + c_2 \left(\frac{\eta_m - \left(\frac{Q_{om2}}{Q_{im}} \right)_{ref}}{\left(\frac{Q_{om2}}{Q_{im}} \right)_{ref}} \right) + c_3 \left| \min(0, \frac{|\alpha_1 - \alpha_1^{'}|}{\alpha_1^{'}} - 0.25) \right| + \\ & c_4 \left| \min(0, \frac{|\alpha_2 - \alpha_2^{'}|}{\alpha_2^{'}} - 0.25) \right| + c_5 \left| \min(0, \frac{|L - L^{'}|}{L^{'}} - 0.25) \right| + c_6 \left| \min(0, \frac{|I_1 - I_1^{'}|}{I_1^{'}} - 0.25) \right| + \\ & c_7 \left| \min(0, \frac{|I_2 - I_2^{'}|}{I_2^{'}} - 0.25) \right| + c_8 \left| \min(0, \frac{|I_2 - I_2^{'}|}{I_2^{'}} - 0.25) \right| + c_9 \left| \min(0, \frac{|I_4 - I_4^{'}|}{I_4^{'}} - 0.25) \right| \end{aligned} \tag{2}$$

where c_1, c_2, c_3, c_4, c_5, c_6, c_7, c_8, c_9 are the weights (According to the degree of influence of each factor, these weights are set c_1=c_2=0.2, $c_3 = c_4 = 0.1, c_5 = c_6 = c_7 = c_8 = c_9 = 0.08$), P_{out2} the intake outlet total pressure, P_{in} the inlet total pressure, Q_{om2} the intake outlet airflow rate, Q_{im} the inlet airflow rate.

Surrogate model

Due to its great nonlinear fitting capability, the back-propagation multi-layer feed forward artificial neural network (BP-MLFANN) is usually used to approximate the complicated nonlinear relationships of practical problems. During the training process, the dataflow is controlled by Eq. (4), the linear function as the activation function for the input and output layers, the Sigmoid function shown in Eq.(5) used for the hidden layer, and the error between the practical output value and the ideal output value presented by Eq.(6).

$$u_j = \sum_{i=1}^{n} \omega_i x_i + \theta_j \tag{4}$$

$$y_j = f(u_j) = 1 \Big/ \left(1 + \exp(-u_j)\right) \tag{5}$$

$$E_{AV} = \frac{1}{N} \sum_{n=1}^{N} E(n) = \frac{1}{2N} \sum_{n=1}^{N} \sum_{j=1}^{T} \left(d_j(n) - y_j(n)\right)^2 \tag{6}$$

where x denotes the input data, u the data of hidden-layer neuron, ω the weight coefficient, θ the biases value, y and d respectively the actual output value and the ideal output value, E_{AV} the total average error, T and N the total number of output elements and the number of iterations respectively.

The approximation precision of BP-MLFANN is easily affected by its topology structure. However, there is no mature specific theory to determine the topology of MLFANN accurately and effectively. To get an appropriate topology of BP-MLFANN automatically, a hybrid intelligent algorithm is proposed in which in which it combines the quick searching capability of hybrid particle swam optimization (HPSO) and the ability to quickly jump out the local optimum of a modified very fast simulated annealing algorithm (MVFSA). The hybrid particle swarm optimization is included by the continuous particle swam optimization (CPSO) and the discrete particle swam optimization (DPSO). The definition formulas of its update velocity and location for CPSO are shown in Eqs. (7, 8) and the update velocity and position of DPSO can be controlled by Eqs.(7, 9). For the MVFSA, the initial particle is distributed by Eq.(10), and the random probability of acceptance P_r is defined based on Boltzmann-Gibbs distribution shown in Eq.(11).

$$v_{i,j}^{1}=\left(\frac{2}{\left|2-C-\sqrt{C^2-4C}\right|}\right)\left[\begin{array}{l}\left(\left(\mu_{\min}+(\mu_{\max}-\mu_{\min})*\gamma_3\right)+\sigma\cdot N(0,1)\right)v_{i,j}^{0}+\\ c_1\gamma_1\left(P_{i,j}-x_{i,j}^{0}\right)+c_2\gamma_2\left(P_{g,j}-x_{i,j}^{0}\right)\end{array}\right] \tag{7}$$

$$X_{i,j}^{1}=X_{i,j}^{0}+v_{i,j}^{1} \tag{8}$$

$$x_{i,j}=\begin{cases}0 & rand()\le 1-\dfrac{2}{1+\exp\left(-v_{i,j}\right)}\\ x_{i,j} & rand()>1-\dfrac{2}{1+\exp\left(-v_{i,j}\right)}\end{cases}\left(v_{i,j}<0\right)\ or\ \begin{cases}1 & rand()\le \dfrac{2}{1+\exp\left(-v_{i,j}\right)}-1\\ x_{i,j} & rand()>\dfrac{2}{1+\exp\left(-v_{i,j}\right)}-1\end{cases}\left(v_{i,j}>0\right) \tag{9}$$

$$M_{ij}^{'}=M_{ij}+\alpha\cdot B\cdot\left(T_{\max}\exp\left(-ck^{1/N_1}\right)\cdot\operatorname{sgn}\left(u-0.5\right)\left[\left(1+\frac{1}{T_{\max}\exp\left(-ck^{1/N_1}\right)}\right)^{|2u-1|}-1\right]\right) \tag{10}$$

$$P_r=\left[1-(1-h)\cdot\left(E\left(M_{ij}^{'}\right)-E\left(M_{ij}\right)\right)/\left(T_{\max}\exp\left(-ck^{1/N_1}\right)\right)\right]^{1/(1-h)} \tag{11}$$

where v is the particle velocity, two subscripts i, j the particle sequence and the particle vector respectively, C the modified factors and $C=c_1+c_2$, c_1, c_2 the learning factors, $\gamma_1, \gamma_2, \gamma_3$ the random numbers distributed uniformly in $(0,1)$, $P_{i,j}$ the best position in its flight history, $P_{g,j}$ the best position in the particle swarm, μ, σ the average stochastic the inertia weight and the variance of stochastic inertia weight, $N(0,1)$ the random number of the standard normal distribution, $s\left(v_{i,j}\right)$ the mapping value of corresponded velocity, $v_{i,j}$ to the interval $[0,1]$ by Sigmoid function shown in Eq.(9), $x_{i,j}$ the corresponding location, $M_{ij}^{'}$ the disturbed variable, M_{ij} the undisturbed variable, α a positive value and less than 1, B the limitation value of the variable, y_{ij} the Cauchy distribution , h a real number (set h=0.5), E is particle current energy, u a random number ranged from 0 to 1, $T_{\max}$ the initial temperature, N_1 the syllogism coefficient, k the number marked annealing stage and c a given constant and the random probability of acceptance of MVFSA P_r.

Owing to the discrete and continuous characters of the topology of BP-MLFANN, the hybrid intelligent algorithm method is used to optimize the topology structure of BP-MLFANN. The topological optimization includes two procedures such as the numbers of the hidden layers and the neurons per hidden layer are optimized by the DPSO-MVFSA and the weights and biases of neural network are optimized by the CPSO- MVFSA. The evaluation of particle in the DPSO-MVFSA is done based on the results of the CPSO-MVFSA. To ensure the effectiveness of BP-MLFANN, 80% of the sample data is used to train BP-MLFANN and 20% is adopted to verify the prediction accuracy of BP-MLFANN. Four evaluation criteria such as SSE, $RMSE$, R^2, R^2-adj were often used to validate the feasibility of ANN in which SSE and $RMSE$ closer to zero means a smaller random error and a useful prediction, R^2 and R^2-adj closer to one presents a great proportion of variance and a better fit. The fitness function is defined based on the evaluation criteria and shown in Eq. (12).

$$F=C_1\frac{1}{1+\exp\left(-T/200\right)}+C_2\cdot SSE+C_3\cdot RMSE+C_4\cdot R^2+C_5\cdot R^2\text{-adj} \tag{12}$$

Aerodynamic Optimization

Due to the continuous feature of the disturbance of these control parameters, the CPSO-MVFSA is adopted to search the intake grille with optimal aerodynamic performance in the range of the control parameters. The feasibility of CPSO-MVFSA applied to optimize the aerodynamic performance of cascade had been proved in Zhang's work [36]. Since this algorithm can deal with multi-dimension nonlinear optimization problems well, it is used as the aerodynamic optimization algorithm in this work. The whole aerodynamic optimization method is shown in Fig.3.

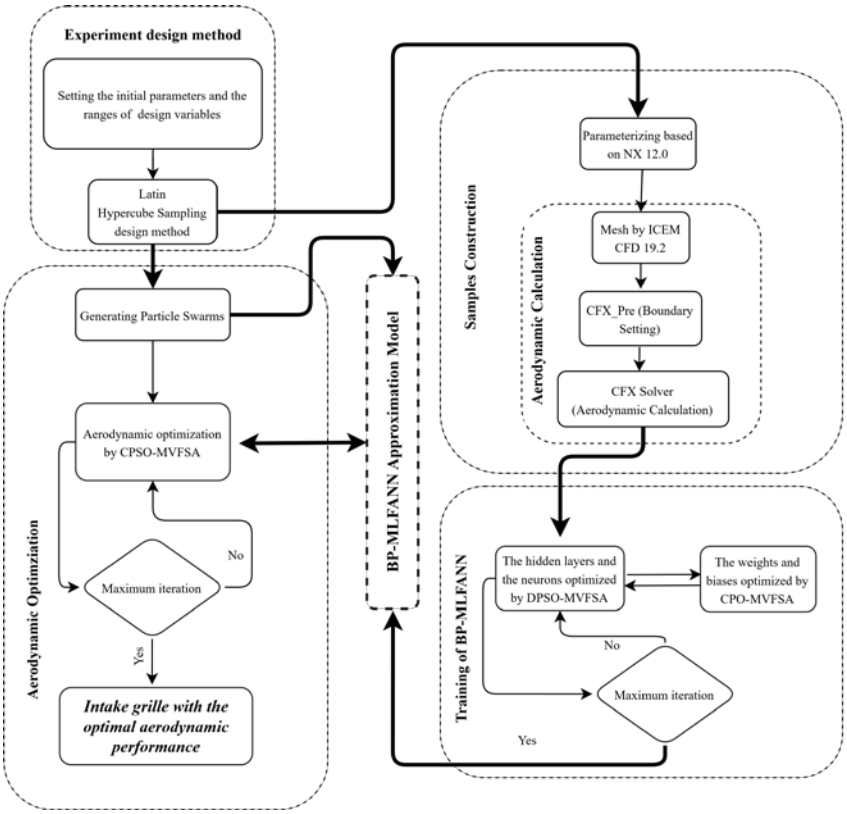

Fig.3 Illustration of Aerodynamic Optimization

AERODYNAMIC OPTIMIZATION OF INTAKE GRILLE

Experiment

The intake grille was designed for the casing impingement cooling of high-pressure turbine (HPT) by drawing airflow from the bypass. And its aerodynamic performance experiments were done in Key Lab. for Power Machinery and Engineering of SJTU. Fig.4 shows the simple illustration of test apparatus in which three total pressure probes and two static pressure probes were mounted, by which the flow rate, the pressure, the total pressure recovery and the intake airflow coefficients could be calculated.

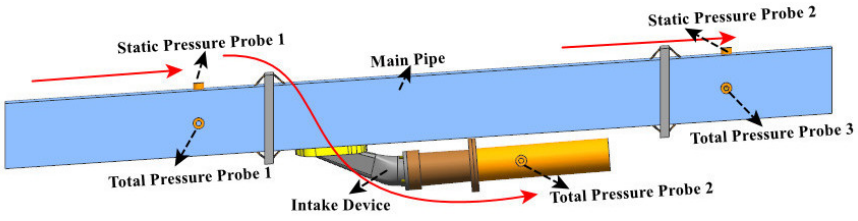

Fig.4 The Test Apparatus of Intake Grille

Simulation and Validation

The aerodynamic performance simulation calculation of the intake grille is done based on the commercial software ANSYS 19.2. Before the calculation, the mesh model shown in Fig.5 is used to present the airflow field and its grids are unstructured by the grid software ICEM 19.2. During the meshing, the grid independence analysis is necessary and five sets of grids are selected to verify the independence. From Fig.6, it is seen that with the increase of the numbers of grids from 1 million to 2.5 million, the total pressure recovery coefficient is gradually increased; and when the number is between 2.5 million and 3 million, the coefficient is barely changed. Thus, the mesh number of this model is set 2.5 million. Since the effects of the boundary layer on this model is required to be considered, the turbulence model, $k-\omega$ which can capture the flow loss of the boundary layer, is used to close the 3-D Reynolds Average Navier-Stokes (RANS) equations. Mass flow and total temperature are selected as the inlet condition and the opening static pressure is composed as the outlet condition.

a) Mesh of test apparatus b) Mesh of intake grille

Fig.5 Mesh Model

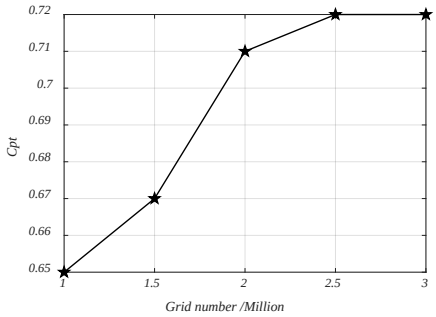

Fig.6 Grid independence analysis (0.4Ma)

During the training of the surrogate model, 300 samples were generated by the Latin Hypercube Sampling design method. To validate the effectiveness of BP-MLFANN, 80% of the sample data is used to train BP-MLFANN and 20% is adopted to verify the prediction accuracy of BP]MLFANN. Four evaluation criteria such as SSE, $RMSE$, R^2, R^2-adj are often used to validate the feasibility of ANN in which SSE and $RMSE$ closer to zero means a smaller random error and a useful prediction, R^2 and R^2-adj closer to one presents a great proportion of variance and a better fit. From table 1, it is found that the prediction accuracy of BP-MLFANN is feasible.

Table 1 Evaluation results

Model	SSE	$RMSE$	R^2	R^2-adj
BP-MLFANN	0.0325	0.0213	0.958	0.916

The intake airflow and the total pressure recovery coefficients corresponding to five design conditions such as 0.25Ma, 0.3Ma, 0.35Ma, 0.4Ma and 0.5Ma, are chosen to evaluate the feasibility of the numerical simulation. It is shown in Fig.7 that there are small gaps between two series of the initial intake grille performance obtained from the experiment and the CFD respectively, such as the maximum intake airflow efficiency error is 2% and the maximum total pressure recovery coefficient error 3%. And the curve trends of these two coefficients obtained from CFD are similar to those of the experiment. Thus, it is believed that the simulation based on CFX is feasible to predict the aerodynamic performance of intake grille.

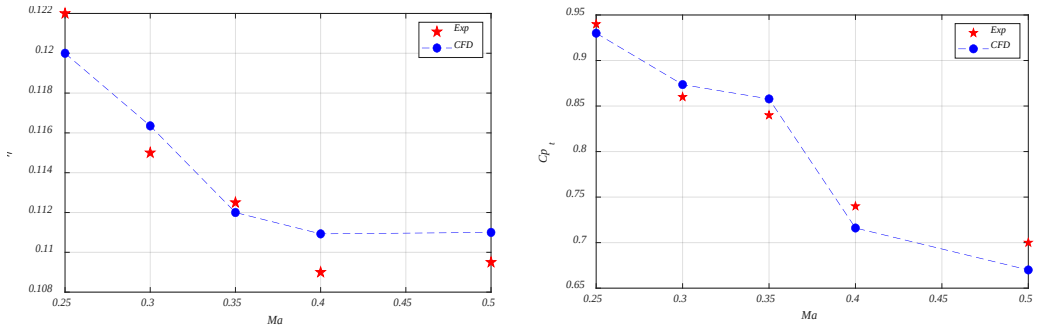

a) Intake airflow coefficient b) Total pressure recovery coefficient

Fig.7 Aerodynamic Performance Validation

Aerodynamic Optimization Analysis

Based on the geometry of initial intake grille, the parameterization is done. Then, utilizing the uniformly distributed aerodynamic samples, BP-MLFANN is trained and used as a surrogate model to predict the fitness value of intake grille. After a series of aerodynamic optimization iterations, the intake grille with optimal aerodynamic performance is found.

To compare the practical differences of the aerodynamic performance, we use the above mentioned five operating conditions to carry out the aerodynamic experiments on these two kinds of grilles such as the original and the optimal intake grilles. According to the collected data, two aerodynamic performance coefficients of the optimal grille are figured

out. And the detailed coefficients of two grilles are displayed in Fig.8. From this figure, it is seen that the average intake airflow and the average total pressure recovery coefficients of the optimized grille are respectively increased by 29.3% and 5.7% in comparisons of those of the initial grille. To more clearly analyze the effects of the geometry changes on the airflow field of the intake grille, one operating condition such as the 0.3Ma, is adopted and simulated by the validated CFD method. In this work, the velocity contours are used as the analytical tool and the detailed contours are shown in Fig.9. In this figure, it can be found that the separation loss of the initial grille is bigger than that of the optimized. Combined with the geometrical differences, it is found that the increase of inlet angle and outlet angle can decrease the airflow separation of the lower surface of each blade and the shrinking of the chord length and the increasing of the interval can enhance the intake airflow. Therefore, the aerodynamic performance of the intake grille can be improved by this aerodynamic optimization method.

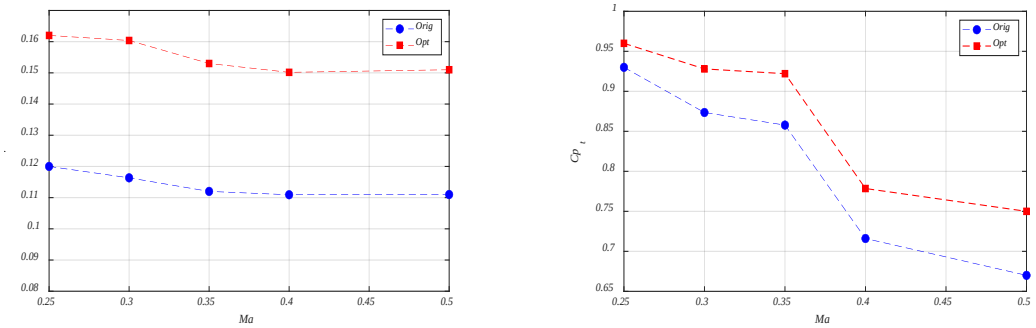

a) Intake airflow coefficient b) Total pressure recovery coefficient

Fig.8 Aerodynamic Performance Comparisons

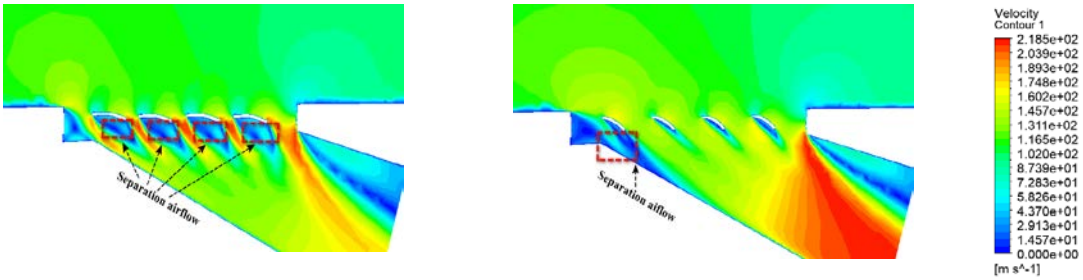

a) Original grille b) Optimized grille

Fig.9 Velocity Contours (0.3Ma)

CONCLUSIONS

In this work, an improved aerodynamic optimization method applied to the intake grille is proposed. The geometry of intake grille is parameterized and a special fitness function is related to its aerodynamic performance and geometrical parameters. An adaptive topological BP-MLFANN is optimized by the HPSO-MVFSA and adopted to evaluate the fitness value of intake grille fast during the optimization process. To verify the feasibility of the improved aerodynamic optimization method, a practical intake grille is chosen to be optimized. Some valuable results can be found as follows.

a) The intake grille is parameterized by seven important geometrical parameters and its shape transformation can be achieved by fewer control parameters in comparison of the experience design. Simultaneously, this method has the enough flexibility to cover the important search space.

b) To obtain the fitness value of intake grille fast during the optimization process, the BP-MLFANN is used as a surrogate model to predict the fitness value of intake grille. The topology structure of BP-MLFANN is optimized by the HPSO-MVFSA adaptively. Through this model, the effect of human factors on the training of BP-MLFANN can be decreased and the approximation capability of the surrogate model can be increased.

c) Through analyzing the results from the practical intake grille, it is obtained that the average intake airflow and the average total pressure recovery coefficients of the optimized grille are respectively increased by 29.3% and 5.7% in comparisons of those of the initial grille and the separation loss of the optimized grille is smaller than that of the original. Thus, it is believed that this aerodynamic optimization can be used to optimize the aerodynamic performance of intake grille.

ACKNOWLEDGMENTS

This research was supported by no fund.

REFERENCES

Da Soghe R., Andreini A. (2011). Numerical Characterization of Aerodynamic Losses of Jet Arrays for Gas Turbine Applications. *Journal of Engineering for Gas Turbines and Power*, 134.5(2011):110-115. Doi: 10.1115/GT2011-46212.

Dominic A. Masters, Nigel J. Taylor, Thomas Rendall, Christian B. Allen, Daniel J. Poole. (2003). Review of airfoil Parameterization Methods for Aerodynamic Shape Optimization. AIAA paper 2015-0761, *Proceedings AIAA Science and Technology Forum*, Kissemee, Florida.

Duan, W., An, L. Q., Wang, Z. (2017). Strength reliability analysis of turbine blade using surrogate models research. *Journal of Applied Sciences Engineering and Technology*, Vol. 7(18), pp. 3699-3708. Doi: 10.19026/rjaset.7.724.

Gu Wei，Qiao Jian，Chen Xiao，Liu Yu-fang. (2013). A Review of Turbine Clearance Control System for Civil Turbofan Engine. *Gas Turbine Technology*, 26(1). Doi: 10.16120/j.cnki.issn1009-2889.2013.01.003

Lattime S. B., Steinetz B. M. (2012). High-Pressure-Turbine Clearance Control Systems: Current Practices and Future Directions. *Journal of Propulsion & Power*, 20(2):302-311. Doi: 10.2514/1.9255

Melcher K. J. (2003). Controls considerations for turbine active clearance control. *NASA seals & secondary flow workshop*, 2003-11-5.

Nazghelichi, T., Aghbashlo, M., Kianmehr, M. H. (2011). Optimization of an artificial neural network topology using coupled response surface methodology and genetic algorithm for fluidized bed drying. *Computers & Electronics in Agriculture*, Vol. 75(1), pp. 84-91. Doi: 10.1016/j.compag.2010.09.014.

Tapanlis, O, Choi, M, Gillespie, DRH, Lewis, LV, & Ciccomascolo, C. (2014). The Effect of Impingement Jet Heat Transfer on Casing Contraction in a Turbine Case Cooling System. ASME paper：V05BT14A018，*Proceedings of the ASME Turbo Expo 2014: Turbine Technical Conference and Exposition. Volume 5B: Heat Transfer. Düsseldorf*, Germany, June 16–20. Doi: 10.1115/GT2014-26749.

Zeng Jun, Wang Peng-fei. (2012). Analysis on turbine active clearance control technology of civil aircraft engine. *Journal of Aeronautical Science and Technology*, 134(2) :1-6. Doi: 10.3969/j.issn.1007-5453.2012.02.003

Zhihui Li, and Xinqian Zheng. (2017). Review of design optimization methods for turbomachinery aerodynamics. *Progress in Aerospace Sciences*, Vol. 93, pp. 1-23. Doi: 10.1016/j.paerosci.2017.05.003.

Zhengqiu Yang, Yapei Cao and Jiapeng Xiu. (2014). Power generation forecasting model for photovoltaic array based on generic algorithm and BP neural network. *2014 IEEE 3rd International Conference on Cloud Computing and Intelligence Systems*, pp. 380-383, Doi: 10.1109/CCIS.2014.7175764.

Zhang J R., Zhang J., Lok T M. (2007). A hybrid particle swarm optimization–back-propagation algorithm for feedforward neural network training. *Applied Mathematics & Computation*, 185(2), pp. 1026-1037. Doi: 10.1016/j.amc.2006.07.025.

Zhang S., Yang B., Xie H. Song M. (2020). Applications of an Improved Aerodynamic Optimization Method on a Low Reynolds Number Cascade, *Processes*, Vol.8. Doi: 10.3390/pr8091150.